Available online at www.sciencedirect.com
ScienceDirect
International Journal of Heat and Mass Transfer 51 (2008) 4461–4469
International Journal of HEAT and MASS TRANSFER
www.elsevier.com/locate/ijhmt

# Bubble oscillation on thin wire during subcooled boiling

J.F. Lu, X.F. Peng *

*Laboratory of Phase-change and Interfacial Transport Phenomena, Department of Thermal Engineering, Tsinghua University, Beijing 10084, China*

Received 5 April 2007; received in revised form 19 November 2007
Available online 24 March 2008

**Abstract**

An experimental investigation was conducted to observe bubble oscillation phenomenon on heating wires during subcooled pool boiling, and associated analyses were proposed to describe these dynamical processes. Single bubble oscillation usually occurred between two immobile bubbles regularly, and coupling bubble oscillation with two oscillating bubbles can be also observed in some special conditions. Both experimental evidences and theoretical analyses indicated that the interfacial thermocapillary effect and the interaction of adjacent bubbles played the principle roles in bubble oscillation. The evolution of bubble oscillation was mainly affected by the effective viscosity, and the oscillation would weaken for positive effective viscosity and magnify for negative effective viscosity. The oscillation near the equilibrium point can be handled as a harmonic oscillation. The coupling oscillation was also investigated by the dynamical model, and its characteristics were similar to those of single bubble oscillation. The theoretical predictions were compared with experimental results and showed a reasonable agreement with each other.


*Keywords:* Pool boiling; Bubble oscillation; Bubble dynamics; Thermocapillary force; Thin wire

## 1. Introduction

In the last decade, complex bubble dynamics and nonlinear phenomena in boiling system have been investigated in many available articles. Shoji et al. [1,2] investigated nonlinear bubble dynamics and chaos in boiling system. Wu and Cheng [3] measured periodic oscillations of wall temperature, inlet and outlet water temperatures and pressures, and instantaneous mass flux in boiling system. Buyevich and Natalukha [4] investigated self-oscillating regimes of nucleate, transition and film boiling. As one of the most successful applications of boiling phenomenon to the microelectromechanical systems (MEMS), thermal ink jet printer used bubble expansion as driving force [5], and bubble dynamics of expansion and oscillation is of critical importance for controlling print quality. Meanwhile, bubble sliding phenomena were also investigated as significant phenomena and processes in various boiling systems [6,7].

Takahashi et al. [8] investigated the bubble oscillation by using a vapor bubble on thin film micro heater, and noted that one of driving forces might be the thermocapillary force caused by surface tension gradient due to the temperature distribution along the bubble interface. Wang et al. [9] conducted a series of subcooled boiling experiments on very thin Pt wires, and observed many interesting phenomena, such as bubble forward-and-backward motion and jet flows. Our previous work [10] proposed a theoretical model to describe the dynamical characteristics of bubble separation and collision phenomena during subcooled boiling of water on thin heating wires, and indicated the physical significance of the interfacial thermocapillary force and the interaction between neighbor bubbles. Though these available investigations provided some important experimental evidences, the characteristics of bubble oscillation was not understood very well.

This paper mainly presents experimental observation and theoretical analyses for bubble oscillation on very thin

* Corresponding author. Tel./fax: +86 10 6278 9751.
*E-mail address:* pxf-dte@mail.tsinghua.edu.cn (X.F. Peng).

0017-9310/$ - see front matter © 2008 Elsevier Ltd. All rights reserved.
doi:10.1016/j.ijheatmasstransfer.2007.12.025

**Nomenclature**

| | |
|---|---|
| $A$ | amplitude (m) |
| $a$ | acceleration (m s$^{-2}$) |
| $B$ | tension gradient with temperature (J m$^{-2}$ K$^{-1}$) |
| $D$ | temperature gradient (K m$^{-1}$) |
| $l$ | distance (m) |
| $q$ | heat source (W) |
| $q'$ | linear heat source (W m$^{-1}$) |
| $R$ | radius (m) |
| $T$ | temperature (K), period (s) |
| $t$ | time (s) |
| $u$ | velocity (m s$^{-1}$) |
| $\omega$ | angular frequency (s$^{-1}$) |
| $\mu$ | effective viscosity (N s m$^{-3}$) |
| $\varepsilon$ | relative viscosity (–) |

*Subscripts*

| | |
|---|---|
| 0 | initial or reference state |
| b | bubble |
| e | equilibrium |
| l | liquid |
| m | maximum velocity |
| w | wire |

*Greek symbols*

| | |
|---|---|
| $\alpha$ | dimensionless coefficient (–) |
| $\lambda$ | heat transfer coefficient (W m K$^{-1}$) |

heating wires during subcooled pool boiling at moderate heat fluxes. Experimental results showed that the bubble oscillation was mainly driven by thermocapillary force and affected by neighbor bubbles, and ideal models were proposed to investigate the dynamic characteristics of bubble oscillation in order to understand the mechanism.

## 2. Experimental observation

### 2.1. Experiment facility

The experimental facility employed in this investigation mainly included three parts, or the test section, power supplier and acquisition system, as illustrated in Fig. 1. The test module was a vessel having size of $250 \times 250 \times 400$ mm$^3$ (length $\times$ width $\times$ height) (1) and made of stainless steel. There were two glass windows opened oppositely on two sides. Two copper electrodes (2) of diameter 5 mm were installed on the cover, and a wire heater inside the vessel was horizontally connected to two electrodes. The wire heaters were made of platinum, and were about 80–100 mm long with diameter of 100 μm. A pre-heater (3) and cooler (4) were applied to control and adjust the bulk liquid temperature. The pressure in the present experiments was kept at the atmospheric pressure.

The power supplier (5) was a HP Agilent Model-6031A system, which can provide a maximum voltage of 20 V and maximum power of 1000 W. A uniform heat flux applied by direct current in the wire was generated to heat the liquid. To reduce the boundary effect of electrodes, the tested section was selected as the middle region of wire, and the voltage of the tested section was measured by a voltage gauge (6) directly. The experiments employed pure water as working fluid.

The acquisition system included image acquisition and data acquisition systems, and a personal computer (7) was used to record the images and data. The photographic system consisted of a high-speed CCD camera (the Motionscope PCI, Redlake imaging) (8), a high-resolution image acquisition card, and zoom lenses. The CCD camera can reach a high speed up to 2000 frames per second. The present experiments used the speed of 500 fps, and the resolution was $320 \times 280$ pixels. In this investigation, the image field was about $4 \times 4$ mm$^2$, and a pixel was about $12 \times 12$μm$^2$.

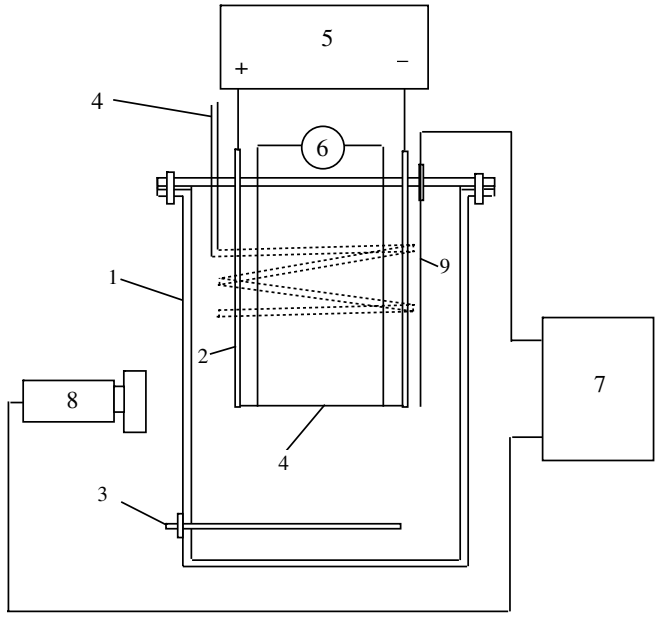


Fig. 1. Schematics of testing system: (1) testing vessel, (2) electrodes, (3) preheater, (4) cooler, (5) power supply, (6) voltage gauge, (7) personal computer, (8) CCD camera, (9) thermocouple.

The bulk liquid temperature was directly measured by T-type thermocouple (9) placed in the bulk liquid as Fig. 1, and the uncertainty of the thermocouple was 0.2 K. The current and voltage of the test section were measured to determine the applied heat flux and average wire temperature. The resistance of the wire was approximately

a linear function of the wire temperature, and was used to estimate the average wire temperature. An error analysis showed the overall uncertainty of the average wire temperature measurement was 2 K, while the uncertainty of the heat flux was less than 1%. For complex bubble motions in boiling system, their dynamic characteristics were mainly determined by the local temperature and other conditions instead of the average wire temperature.

### 2.2. Bubble oscillation

Bubble oscillation usually occurs at bulk liquid temperature of 20–40 °C and moderate heat flux 1.2–2 × $10^6$ W $m^{-2}$. In present experiments, bubbles can oscillate between immobile bubbles or some ends on a wire, and single bubble oscillation usually occurs between two immobile bubbles regularly. Additionally, an oscillating bubble on wires mostly moves at a maximum speed of 20–80 mm/s, and its spatial period is about 0.3–2 mm. These different experimental observations and their associated experimental conditions will be presented and discussed in followings.

Fig. 2 presents a typical process of a single bubble oscillation for boiling of water at bulk liquid temperature of 30°C and heat flux of 1.5 × $10^6$ W $m^{-2}$. Two large bubbles stood on their initial positions and a small bubble with diameter of 0.10 mm oscillated between them. The small bubble oscillated with an average velocity of 20–30 mm/s, and it returned to the initial location after 0.026 s. Additionally, the oscillation period was about 0.026 s, and the spatial period was about 0.6 mm, which was about six times of the bubble diameter.

Fig. 3 presents two bubble oscillations nearby for boiling of water at bulk liquid temperature of 30 °C and heat flux of 1.6 × $10^6$ W $m^{-2}$. At initial time, two bubbles were both near the center immobile bubble. In the next 0.014 s, the two bubbles both slipped away from the center bubble.

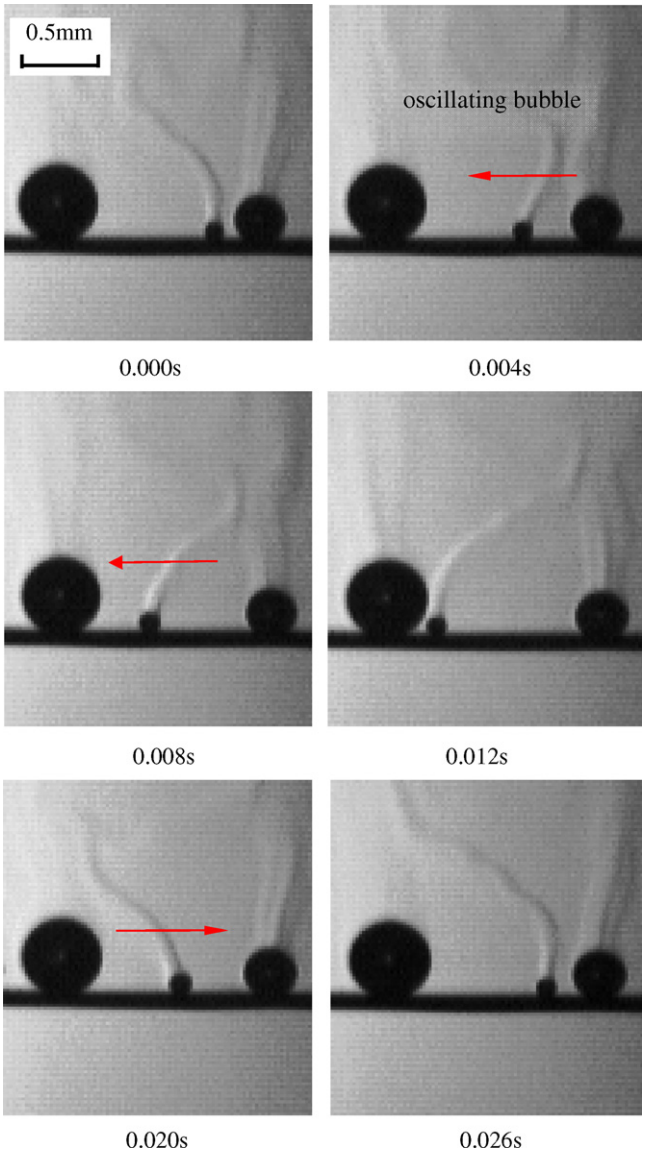


Fig. 2. Single bubble oscillation ($T_{liq}$ = 30 °C, $q''$ = 1.5 × $10^6$ W $m^{-2}$, $T_w$ = 102 °C).

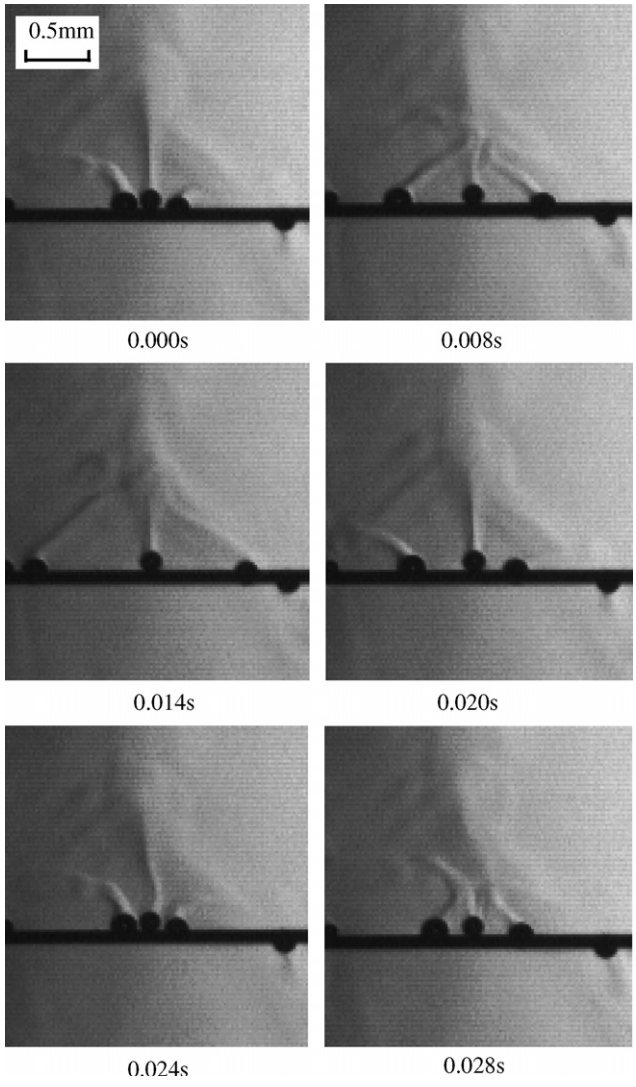


Fig. 3. Two bubble oscillations with center bubble ($T_{liq}$ = 30 °C, $q''$ = 1.6 × $10^6$ W $m^{-2}$, $T_w$ = 105 °C).

At 0.024 s, the two moving bubbles returned to their initial places. In 0.028 s, the two bubbles began to separate from the center bubble again. In special conditions, two bubbles may oscillate between two immobile bubbles without any center bubble as Fig. 4 and this phenomenon is termed as coupling bubble oscillation.

For a bubble oscillation process, it usually ends in two ways. If the oscillating bubble moves faster as time going, it will probably coalesce with the immobile bubble or make the immobile bubble unstable through collision. If the bubble oscillation weakens as time going, the oscillating bubble will usually halt near the center of the two immobile bubbles in the end.

Fig. 5 presents a bubble oscillation process for boiling of water at bulk liquid temperature of 30 °C and heat flux of $1.6 \times 10^6$ W m$^{-2}$. At initial time, the bubble oscillated between two immobile bubbles, its period was about 0.054 s. After that, the amplitude of the bubble oscillation magnified, until it coalesced with the left immobile bubble at 0.168 s, which was about three periods later.

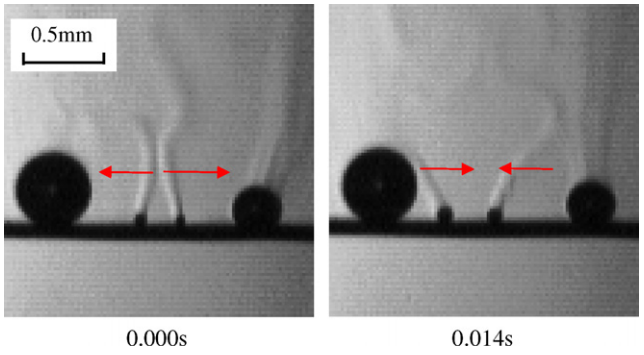


Fig. 4. Coupling bubble oscillation ($T_{liq} = 30$ °C, $q'' = 1.6 \times 10^6$ W m$^{-2}$, $T_w = 105$ °C).

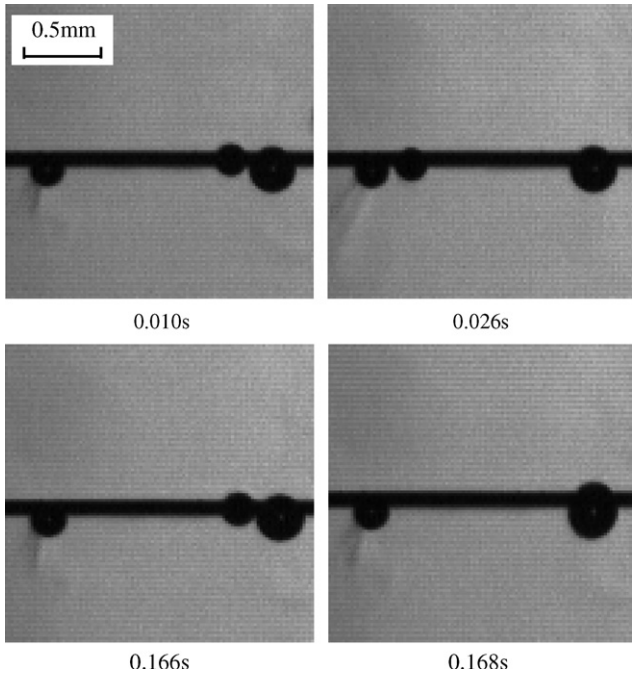


Fig. 5. Bubble coalesce after oscillation ($T_{liq} = 30$ °C, $q'' = 1.6 \times 10^6$ W m$^{-2}$, $T_w = 105$ °C).

Typically, the simple oscillation with a single moving bubble as shown in Fig. 2 occurred at bulk liquid temperature of 30 °C and heat flux under $1.55 \times 10^6$ W m$^{-2}$, while the complex oscillation with several moving bubbles as shown in Figs. 3 and 4 occurs at heat flux above $1.55 \times 10^6$ W m$^{-2}$. In Fig. 5 the oscillation with one moving bubble was unstable because the heat flux was above $1.55 \times 10^6$ W m$^{-2}$.

Generally, the spatial period of the bubble oscillation is usually 3–10 times diameter of the oscillating bubble, while the interaction range between immobile bubbles is usually less than three times their diameter [11]. As a result, the oscillating bubble can strengthen the interaction of immobile bubbles far away, and then it will enhance the heat transport due to its movement and associated phenomena.

## 3. Basic bubble oscillation dynamics

### 3.1. Temperature profile of a two immobile bubble system

The thermocapillary force can cause liquid convection from higher to lower temperature region along the interface and generates a force on the bubble towards the higher temperature region. For subcooled boiling on thin wires, the temperature near the oscillating bubble should be affected by the adjacent bubbles due to their growth and heat absorbing. In addition, the thermocapillary force and the adjacent bubbles were expected to be important effects for bubble oscillation in this investigation.

To investigate the bubble oscillation, consider a system containing two immobile bubbles on a heating wire horizontally installed, as shown in Fig. 6. In present investigation, the immobile bubbles are usually assumed equivalent, and that does not affect the basic oscillation characteristics. The wire is treated as a line heat source with uniform heat generation. The two immobile bubbles, having the same radius of $r_b$, serve as heat sinks locating at $-l$ and $l$. Additionally, a single bubble oscillates between these two immobile bubbles on the wire.

Since the system in Fig. 6 is simplified to a system with a line heat source and two heat sinks, the steady temperature of the liquid is

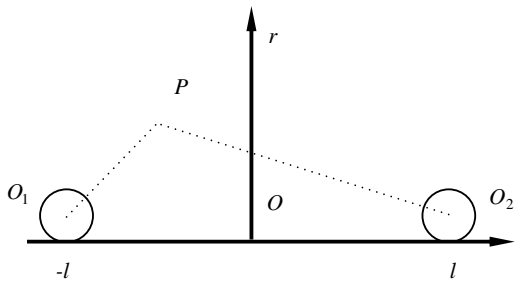


Fig. 6. Analytical model for two immobile bubbles system.

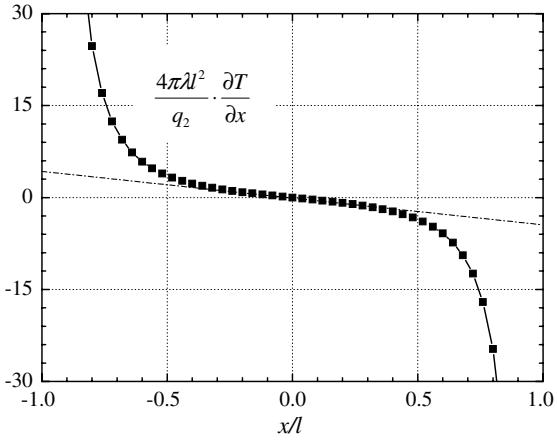


Fig. 7. Temperature gradient distribution for single bubble oscillation.

$$T = -\frac{q_2}{4\pi\lambda\overline{O_1P}+} - \frac{q_2}{4\pi\lambda\overline{O_2P}} + \frac{q_1'}{2\pi\lambda}\ln r + C_0 \tag{1}$$

where $q_1'$ denotes the heat generation per unit length of the wire, and $q_2$ denotes the heat generation of immobile bubbles, $\lambda$, heat transfer coefficient including conductivity and convection [10]. The first two items on the right side of Eq. (1) are caused by the two sinks, respectively, the third item is caused by the line source, and the last item $C_0$ is a constant dependent upon the boiling conditions.

For a single small bubble oscillation between two immobile bubbles on the wire, an arbitrary point $P$ along the bubble track is very close to the wire, and both $O_1P$ and $O_2P$ have small angle with the wire. Therefore, both $\overline{O_1P} \approx x + l$ and $\overline{O_2P} \approx l - x$ are acceptable approximations. The temperature of the liquid close to the wire between two bubbles is

$$T = -\frac{q_2}{4\pi\lambda(x+l)} - \frac{q_2}{4\pi\lambda(l-x)} + C \tag{2}$$

where $C = \frac{q_1'}{2\pi\lambda}\ln(r_w + r_b) + C_0$.

So the local temperature gradient is obtained as,

$$\frac{\partial T}{\partial x} = \frac{q_2}{4\pi\lambda l^2}\left[\frac{1}{(x/l+1)^2} - \frac{1}{(1-x/l)^2}\right] \tag{3}$$

Near to the center or $x \approx 0$, the temperature gradient linear approximates to

$$\frac{\partial T}{\partial x} = -\frac{q_2 x}{\pi\lambda l^3} \tag{4}$$

There are three regions between the two immobile bubbles: linear region near to $x = 0$, two nonlinear regions near immobile bubbles in Fig. 7.

### 3.2. Basic bubble oscillation characteristics

The thermocapillary effect was noted as an important factor in the liquid flow and bubble motion [12–14], and our previous work [10] proposed a theoretical model to describe the bubble dynamical characteristics. The dynamical equation of a moving bubble with radius $R$ on a heating wire can be expressed as [10]

$$\frac{2}{3}\pi\rho_l R^3 a = -6\pi\mu R u + \frac{8}{3}\pi\alpha D B R^2 \tag{5a}$$

or

$$a = -ku + c \tag{5b}$$

where $k = \frac{9\mu}{\rho_l R^2}$ is relative viscosity, $c = \frac{4\alpha BD}{\rho_l R}$ acceleration caused by external thermocapillary force, $\alpha$, denotes nondimensional coefficient, $D$ means external temperature gradient. The effective viscosity force [10,16] includes the viscous force and thermocapillary force caused by the bubble motion. The parameter $\alpha$ [10] means the ratio of the interface temperature gradient and the bulk temperature gradient, and it is determined by the interfacial condition and local heat transfer. From Eq. (5), the oscillation process has different dynamic characteristics according to different effective viscosity $\mu$.

First, consider the oscillation with $\mu \approx 0$, and Eq. (5), evolves to

$$a \approx \frac{4\alpha BD}{\rho_l R} \tag{6}$$

In fact, the effective viscosity usually does not play an important role in one or half period, so the dynamic characteristics of oscillation in half period are similar with each other. Substituting Eq. (3) into Eq. (6) yields

$$\frac{d^2x}{dt^2} = \frac{4\alpha B}{\rho_l R}\left(\frac{q_2}{4\pi\lambda(x+l)^2} - \frac{q_2}{4\pi\lambda(x-l)^2}\right) \tag{7}$$

Using the initial condition as $u = 0$ for $x_0 < 0$, integrating Eq. (7) yields

$$u^2 = \frac{8\alpha B}{\rho_l R}\cdot\frac{q_2}{4\pi\lambda}\left[\left(\frac{1}{x_0+l} - \frac{1}{x+l}\right) - \left(\frac{1}{x_0-l} - \frac{1}{x-l}\right)\right] \tag{8}$$

The bubble oscillates between $x_0$ and $-x_0$, and the oscillation process can continue for a long time. At $x = 0$, the oscillating bubble attains its maximum velocity as

$$u_m = \left(\frac{8\alpha B}{\rho_l R}\frac{q_2}{4\pi\lambda}\right)^{1/2}\left(\frac{1}{x_0+l} - \frac{1}{x_0-l}\right)^{1/2} \tag{9}$$

The bubble oscillating velocity in Fig. 2 is illustrated in Fig. 8, $l = 0.56$ mm, $x_0 = -0.30$ mm, $x_0/l = -0.54$. In addition, the predict results from Eqs. (8) and (9) with $u_m = 68$ mm s$^{-1}$ is illustrated as the line in Fig. 8. As a conclusion, the theoretical results are compared with experimental results very well.

In half oscillation period, the predicted time from Eq. (9) can be integrated as

$$t(x) - t_0 = \int_0^x dx/u \tag{10}$$

where $t_0$ means the time at the center or $x = 0$. Consider experimental results in Fig. 2 and the predicted conditions in Fig. 8, and the oscillating time of experimental and

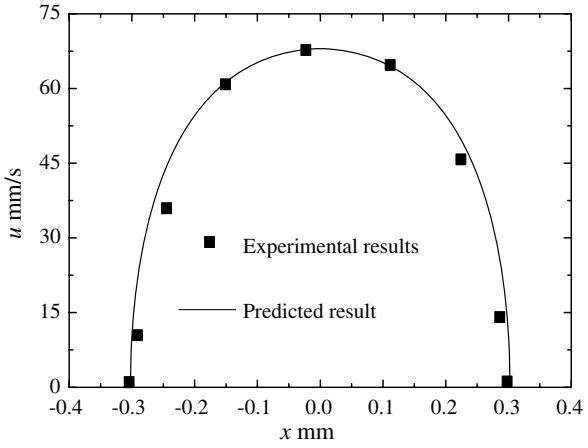


Fig. 8. Experimental and theoretical oscillating velocity.

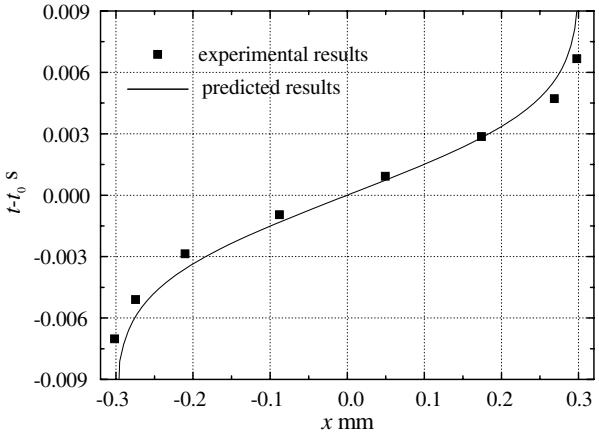


Fig. 9. Theoretical and experimental oscillating process.

predicted results are illustrated in Fig. 9. Obviously, the predicted results have a good agreement with the experimental results except two boundary regions.

## 4. Bubble oscillations with various effective viscosity

### 4.1. Oscillation with positive effective viscosity

For the oscillation with $\mu \approx 0$, it can continue for enough long time, and its dynamic characteristics are the same as that in half period. However, the oscillations usually halt or magnify during 0.1–2 s in practical experiments, and that is mainly caused by non-zero effective viscosity. In previous investigation [16], the effective viscosity $\mu$ will be positive when the bubble absorbs heat slowly, while the effective viscosity would be negative when the bubble absorbs heat quickly at high heat flux.

Substituting Eq. (3) into Eq. (5), yields

$$\frac{\mathrm{d}^2x}{\mathrm{d}t^2}+\frac{9\mu}{\rho_1R^2}\frac{\mathrm{d}x}{\mathrm{d}t}-\frac{4\alpha B}{\rho_1R}\frac{q_2}{4\pi\lambda}\left[\frac{1}{(x+l)^2}-\frac{1}{(x-l)^2}\right]=0 \qquad (11a)$$

or

$$\frac{\mathrm{d}^2(x/l)}{\mathrm{d}t^2}+\frac{9\mu}{\rho_1R^2}\frac{\mathrm{d}(x/l)}{\mathrm{d}t}-\frac{4\alpha B}{\rho_1R}\frac{q_2}{4\pi\lambda l^3}\left[\frac{1}{(x/l+1)^2}-\frac{1}{(x/l-1)^2}\right]=0 \qquad (11b)$$

As the effective viscosity is positive $\mu > 0$, the oscillation will weaken and the oscillating bubble will stop at a certain position at last. Corresponding to an oscillation system similar to Fig. 2, $R = 0.06$ mm, $l = 0.56$ mm, $x_0 = -0.30$ mm, $\rho_1 \approx 1000$ kg m$^{-3}$, $B \approx 1.7 \times 10^{-4}$ N m$^{-1}$ K$^{-1}$, and then the whole oscillation process from Eq. (11) with $\mu \approx 4.6 \times 10^{-6}$ N s m$^{-1}$ and $\frac{\alpha q_2}{4\pi\lambda} = 4.5 \times 10^{-5}$ K m$^{-1}$ is illustrated in Fig. 10. Obviously, the oscillation weakens as time going in Fig. 10a, and the amplitude will decrease to half of its initial value within 0.3 s. In the phase diagram of Fig. 10b, there is a stable sink where the oscillating bubble halts.

As the oscillating bubble is very near the center region, the thermocapillary effect can be linearly approximated as Eq. (4), and Eq. (11) evolves to

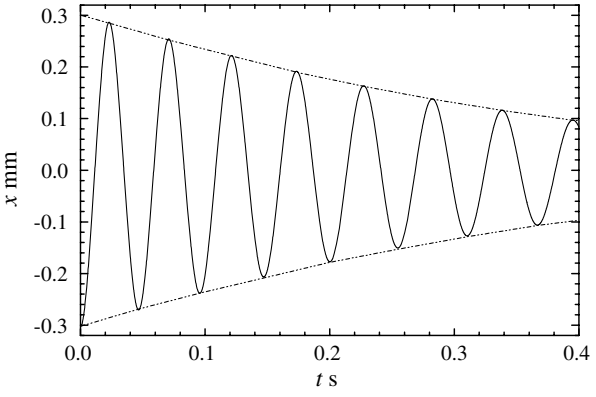


(a) Weakening process

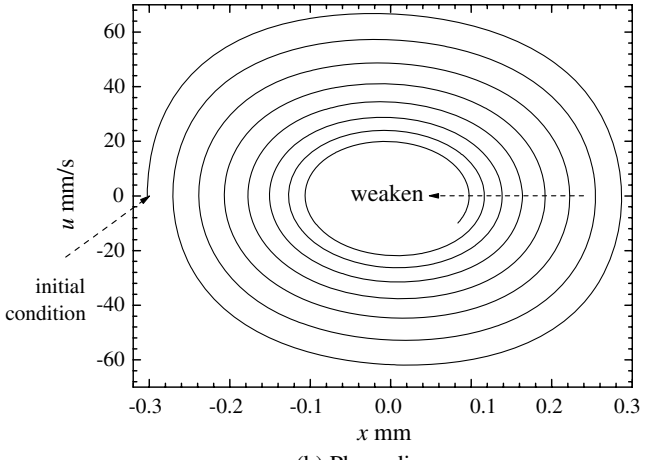


(b) Phase diagram

Fig. 10. Oscillation with positive effective viscosity: (a) weakening process and (b) phase diagram.

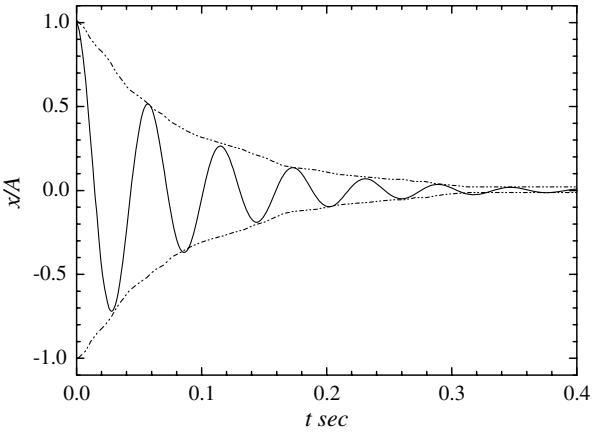


Fig. 11. Attenuation of viscous oscillation.

$$\frac{d^2x}{dt^2}+\frac{9\mu}{\rho_1 R^2}\frac{dx}{dt}+\frac{16\alpha B}{\rho_1 R}\frac{q_2}{4\pi\lambda l^3}x=0 \tag{12}$$

The evolution with effective viscosity is simplified as [15]

$$x=A\exp(-kt)\cos[(\omega_0^2+k^2)^{1/2}t+\beta] \tag{13}$$

where $A$ and $\beta$ are the initial amplitude and phase angle, and the harmonic oscillation angle frequency $\omega_0=(\frac{16\alpha B}{\rho_1 R}\frac{q_2}{4\pi\lambda l^3})^{1/2}$. Consider the previous experimental case in Figs. 2 and 10, and the oscillation process near the origin is illustrated in Fig. 11, here $\beta=0$. Obviously, the oscillation weakens quickly near the origin, and then the bubble will halt.

### 4.2. Oscillation with negative effective viscosity

As the effective viscosity is negative $\mu<0$, the oscillation will magnify and the oscillating bubble may coalesce with an immobile bubble nearby or make the immobile bubble unstable. Corresponding to an oscillation system similar to Fig. 10, the whole oscillation process from Eq. (11) with $\mu=-4.6\times10^{-6}$ N s m$^{-1}$ and $\frac{\alpha q_2}{4\pi\lambda}=4.5\times10^{-5}$ K m$^{-1}$ is illustrated in Fig. 12. Obviously, as oscillation magnifying, the oscillating bubble may contact with the immobile bubble as $|x|=l-R=0.50$ mm, and the oscillation will be unstable. Similar phenomenon can be observed in Fig. 5.

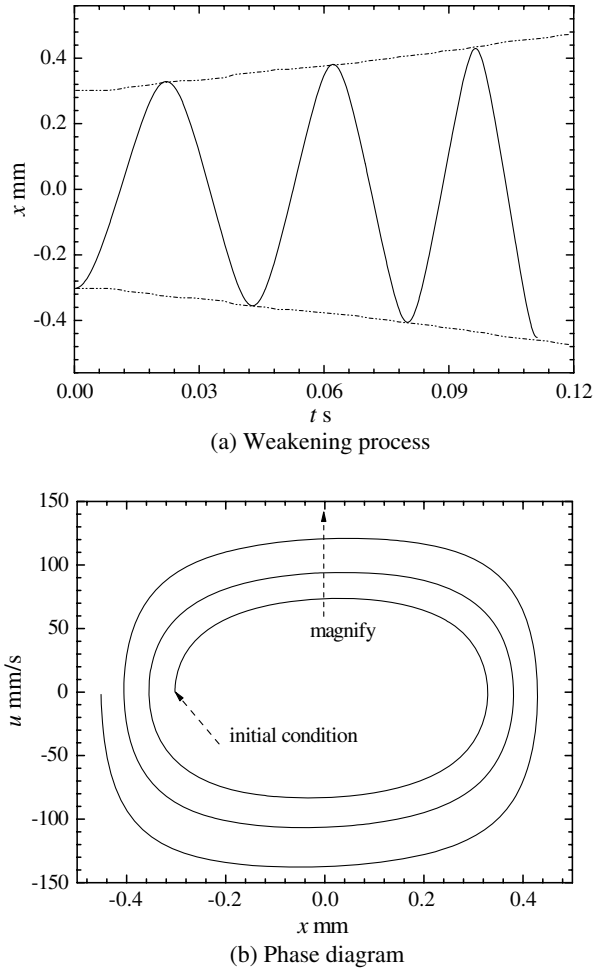


Fig. 12. Oscillation with negative effective viscosity: (a) weakening process and (b) phase diagram.

## 5. Coupling bubble oscillation

Two bubbles may continue oscillating by colliding each other between two immobile bubbles on the wires as Fig. 4. To simplify the analysis, symmetrical coupling oscillation will be investigated and only two adjacent bubbles and the wire is assumed to affect the external temperature field of the oscillating bubble.

For the right oscillating bubble, the local temperature distribution caused by heating wire, the right immobile bubble and left oscillating bubble. For an arbitrary symmetry double bubble oscillation system, the coordinate system as shown in Fig. 13 is employed, and the temperature gradient along $x$-axis is similar to Eq. (3) as

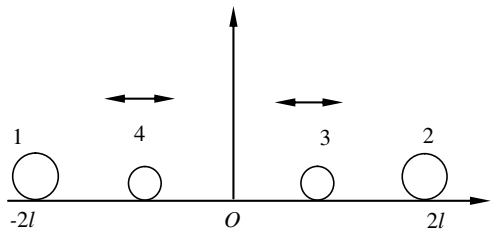


Fig. 13. Coupling bubble oscillation model.

$$\frac{\partial T}{\partial x}=-\frac{q_2}{4\pi\lambda(2l-x)^2}+\frac{q_3}{4\pi\lambda\cdot 4x^2} \tag{14}$$

where $q_2$ denotes the heat generation of immobile bubble, and $q_3$, the heat generation of oscillating bubbles. The temperature gradient from Eq. (14) is shown in Fig. 14, here $q_1\approx q_2$ and $x_e\approx 0.6l$. Similar to Fig. 7, there are three regions: linear region near the equilibrium point, two nonlinear regions far from equilibrium point in Fig. 14.

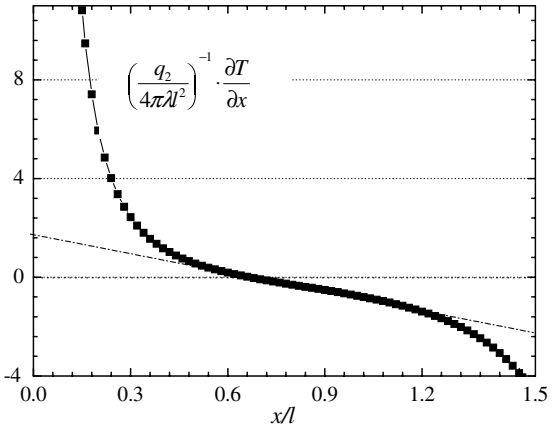


Fig. 14. Temperature gradient distribution for coupling bubble oscillation.

Setting the right side to zero, the position with zero temperature gradient satisfies $(2l - x_e)^2/x_e^2 = 4q_2/q_3$, and then

$$x_e = 2l \cdot [1 + (4q_1/q_2)^{1/2}]^{-1} \tag{15}$$

Substituting Eq. (14) into Eq. (5)

$$\frac{d^2x}{dt^2} + \frac{9\mu}{\rho_l R^2}\frac{dx}{dt} - \frac{4\alpha B}{\rho_l R}\left[-\frac{q_2}{4\pi\lambda(2l-x)^2} + \frac{q_3}{4\pi\lambda\cdot 4x^2}\right] = 0 \tag{16}$$

By ignoring the effective viscosity in one period in Eq. (16), the velocity is

$$u^2 = \frac{8\alpha B}{\rho_l R}\left[\frac{q_3}{16\pi\lambda}\left(\frac{1}{x_0} - \frac{1}{x}\right) + \frac{q_2}{4\pi\lambda}\left(\frac{1}{2l-x_0} - \frac{1}{2l-x}\right)\right] \tag{17}$$

Near the equilibrium position $x_e$, the temperature gradient approximates to

$$\frac{\partial T}{\partial x} = -\frac{1}{2\pi\lambda}\left[\frac{q_2}{(2l-x_e)^3} + \frac{q_3}{4x_e^3}\right]\cdot(x - x_e) \quad x \approx x_e \tag{18}$$

Substituting Eq. (18) into Eq. (5) yields

$$\frac{d^2y}{dt^2} + \frac{27\mu}{4\rho_l R^2}\cdot\frac{dy}{dt} + \frac{8\alpha B}{\rho_l R}\frac{1}{4\pi\lambda}\left(\frac{q_2}{(2l-x_e)^3} + \frac{q_3}{4x_e^3}\right)y = 0 \tag{19}$$

where $y = x - x_e$. The dynamic equation from Eq. (19) is [15]

$$y = A\exp(-kt)\cos[(\omega_0^2 + k^2)^{1/2}t + \beta] \tag{20}$$

where the angle frequency $\omega_0 = \left[\frac{2\alpha B}{\pi\lambda\rho_l R}\left(\frac{q_2}{(2l-x_e)^3} + \frac{q_3}{4x_e^3}\right)\right]^{1/2}$, $A$ and $\beta$ are dependent upon the initial conditions.

Specially for $q_1 = 4q_2$, $x_e = l$, from Eq. (19) yields

$$\frac{d^2y}{dt^2} + \frac{27\mu}{4\rho_l R^2}\cdot\frac{dy}{dt} + \frac{16\alpha B}{\rho_l R}\frac{q_2}{4\pi\lambda l^3}y = 0 \tag{21}$$

Comparing Eq. (21) with (12), their dynamic characteristics are similar.

Generally, the temperature gradient distribution of coupling bubble oscillation is similar to that of single bubble oscillation, and the dynamical characteristics of single and coupling bubble oscillation are also similar.

## 6. Conclusions

Both experimental observation and theoretical analyses were conducted to understand bubble oscillation on very thin heating wires during subcooled boiling. Bubble oscillation phenomenon between two immobile bubbles mostly occurred at moderate heat fluxes. As the experimental evidences and theoretical analyses showed that the interfacial thermocapillary force and the interaction of adjacent bubbles played important roles in bubble oscillation. The basic bubble dynamic equation was proposed to investigate the bubble oscillation, and the dynamic characteristics of the oscillation between two immobile bubbles fitted the experimental results very well. For positive effective viscosity, the oscillation would weaken, while it would magnify for negative effective viscosity. As the oscillating bubble approached to the center, the oscillation can be handled as a harmonic oscillation. The coupling oscillation was also investigated by the dynamic equation, and its characteristics were similar to that of single bubble oscillation. These theoretical conclusions showed a reasonable agreement with experimental results.

## Acknowledgement

This research is currently supported by the National Natural Science Foundation of China (Contract No. 50636030).

## References

[1] M. Shoji, T. Knhno, N. Negishi, S. Toyoshirna, A. Maeda, Chaos in boiling on a small size heater, in: Proceedings of 4th ASME-JSME Thermal Engineering Joint Conference, vol. 2, 1995, pp. 225–232.
[2] M. Shoji, J. Maeda, S. Fujii, Nonlinear bubble dynamics, in: Proceedings of 32th National Heat Transfer Conference, vol. 1, 1995, pp. 257–258.
[3] H.Y. Wu, P. Cheng, Boiling instability in parallel silicon microchannels at different heat flux, Int. J. Heat Mass Transfer 47 (2004) 3631–3641.
[4] Y.A. Buyevich, I.A. Natalukha, Self-oscillating regimes of nucleate transition and film boiling, Int. J. Heat Mass Transfer 39 (1996) 2363–2373.
[5] A. Asai, T. Hara, I. Endo, One-dimensional models of bubble growth and liquid flow in bubble jet printer, Jpn. J. Appl. Phys. 6 (1987) 1794–1801.
[6] K. Cornwell, I.A. Grant, Heat transfer to bubbles under horizontal tubes, Int. J. Heat Mass Transfer 41 (1998) 1189–1197.
[7] G.E. Thorncroft, J.F. Klausner, R. Mei, An experimental investigation of bubble growth and detachment in vertical upflow and downflow boiling, Int. J. Heat Mass Transfer 41 (1998) 3857–3871.
[8] K. Takahashi, J.G. Weng, C.L. Tien, Marangoni effect in microbubble systems, Microscale Them. Eng. 3 (1999) 169–182.
[9] H. Wang, X.F. Peng, B.X. Wang, D.J. Lee, Bubble sweeping and jet flows during nucleate boiling of subcooled liquids, Int. J. Heat Mass Transfer 46 (2003) 863–869.

[10] J.F. Lu, X.F. Peng, Bubble separation and collision on thin wires during subcooled boiling, Int. J. Heat Mass Transfer 48 (2005) 4726–4737.
[11] M. Sultan, R.L. Judd, Interaction of the nucleation phenomena at adjacent sites in nucleate boiling, ASME J. Heat Transfer 105 (1983) 3–11.
[12] T.K. Jun, C.J. Kim, Valveless pumping using traversing vapor bubbles in microchannels, J. Appl. Phys. 83 (1998) 5658–5664.
[13] H. Wang, X.F. Peng, B.X. Wang, D.J. Lee, Bubble-sweeping mechanisms, Sci. Sina, Ser. E 46 (2003) 225–233.
[14] N.O. Young, J.S. Goldstein, M.J. Block, The motion of bubbles in a vertical temperature gradient, J. Fluid Mech. 6 (1959) 350–356.
[15] A.H. Nayfeh, D.T. Mook, Nonlinear Oscillation, Wiley Interscience Publication, 1979.
[16] J.F. Lu, X.F. Peng, Bubble slippage on thin wires during subcooled boiling, Int. J. Heat Mass Transfer 49 (2006) 2337–2346.